QUANTITATIVE FINANCE
RESEARCH CENTRE

UNIVERSITY OF
TECHNOLOGY SYDNEY

QUANTITATIVE FINANCE RESEARCH CENTRE

Research Paper 328 April 2013

Investigating Time-Efficient Methods to Price Compound Options in the Heston Model

Carl Chiarella, Susanne Griebsch and Boda Kang

ISSN 1441-8010 www.qfrc.uts.edu.au

INVESTIGATING TIME-EFFICIENT METHODS TO PRICE COMPOUND OPTIONS IN THE HESTON MODEL

CARL CHIARELLA[♯], SUSANNE GRIEBSCH[⋆] AND BODA KANG[†]

Abstract. The primary purpose of this paper is to provide an in-depth analysis of a number of structurally different methods to numerically evaluate European compound option prices under Heston's stochastic volatility dynamics. Therefore, we first outline several approaches that can be used to price these type of options in the Heston model: a modified sparse grid method, a fractional fast Fourier transform technique, a (semi-)analytical valuation formula using the Green's function of logarithmic spot and volatility and a Monte Carlo simulation. Then we compare the methods on a theoretical basis and report on their numerical properties with respect to computational times and accuracy. One key element of our analysis is that the analyzed methods are extended to incorporate piecewise time-dependent model parameters, which allows for a more realistic compound option pricing.

1. Introduction

The compound option goes back to the seminal paper of Black & Scholes (1973). Not only did they derived their famous pricing formulas for vanilla European call and put options, but they also considered how to evaluate the equity of a company that has coupon bonds outstanding. They argued that the equity can be viewed as a "compound option" because the equity "is an option on an option on $\cdots$ an option on the firm". It was Geske (1979) who first developed a closed-form solution for the price of a vanilla European call on a European call. It turns out that a wide variety of important problems are closely related to the valuation of compound options. Some examples include pricing American puts in Geske & Johnson (1984) and pricing options on portfolios in Seong (2002).

It is well known that derivative securities are not well approximated when it is assumed that the underlying assets follows the geometric Brownian motion process proposed by Black & Scholes (1973). There have been numerous efforts to develop alternative asset return models that are capable of capturing the leptokurtic features found in

Date: Current Version February 19, 2013.

[♯] Corresponding author: carl.chiarella@uts.edu.au; Finance Discipline Group, University of Technology, Sydney, PO Box 123, Broadway, NSW 2007, Australia.
[⋆] susanne.griebsch@uts.edu.au; Finance Discipline Group, University of Technology, Sydney, Australia.
[†] boda.kang@uts.edu.au; Finance Discipline Group, University of Technology, Sydney, Australia.

financial market data, and subsequently to use these models to develop option prices that accurately reflect the volatility smiles and skews found in market traded options. One way to develop option pricing models that are capable of generating such behavior is to allow the volatility to evolve stochastically, in particular using the square-root process introduced by Heston (1993). In this paper, we incorporate this feature into the price of compound options.

In the case of compound options under geometric Brownian motion dynamics, there exist "almost" explicit integral-form solutions. However, in situations involving more general dynamics (such as stochastic volatility), either explicit solutions do not exist or the integrals become difficult to evaluate. In this paper we propose a number of different approaches that can be used to price compound options under Heston (1993) stochastic volatility dynamics. A partial differential equation (PDE) approach is implemented using a modified sparse grid (SG) method. This approach not only provides an efficient and flexible way to compute prices of compound options but it is not only restricted to European-type options but can also include American type or other types of exotic options. We also implement a fractional fast Fourier transform technique, a (semi-) analytic valuation formula using the Green's function of the logarithmic spot and volatility and a Monte Carlo simulation. Then we compare the methods on a theoretical basis and report on their numerical properties with respect to computational times and accuracy.

The remainder of the paper is structured as follows. In Section 2, we outline the framework of the Heston (1993) model, based on which we develop and compare a number of different methods to price compound options. A modified sparse grid approach is discussed in Section 3 to numerically evaluate the partial differential equation that describes the mother option prices. In Section 4 we describe a fractional fast Fourier transform technique that makes use of the representation of the compound option price in terms of its exercise probabilities. Thirdly, we study a (semi-) analytic valuation formula for European compound options by means of the Green's function in Section 5. A Monte Carlo simulation is considered in Section 6 as an alternative pricing method before the efficiency of these approaches is analyzed through a number of numerical tests in Section 7. Finally, we draw some conclusions in Section 8.

2. The Heston Framework and Notation

Following the setting in Heston (1993), the dynamics for the share price S under the risk neutral measure and its variance v are governed by the system of stochastic differential

equations

$$dS_t = (r-q)S_t dt + \sqrt{v_t} S dZ_t^1, \tag{1}$$

$$dv_t = \kappa(\theta - v_t)dt + \sigma\sqrt{v_t} dZ_t^2. \tag{2}$$

Here, the variables r and q denote the rate of interest and the dividend yield, respectively. Their difference is the instantaneous drift of the stock price returns under the risk neutral measure. The stochastic process $\{S_t\}_{t\geq 0}$ followed by the stock price is equivalent to a geometric Brownian motion, but its volatility contains an additional source of randomness. Therefore, the process $\{v_t\}_{t\geq 0}$ represents the instantaneous variance of the spot price with initial variance level $v_0 > 0$. The positive parameters κ, θ and σ denote the speed of mean-reversion, the level of mean-reversion and the volatility of the variance of the Cox-Ingersoll-Ross process. Additionally, the two Wiener processes $\{Z_t^1\}_{t\geq 0}$ and $\{Z_t^2\}_{t\geq 0}$ are correlated

$$\langle dZ_t^1 dZ_t^2 \rangle = \rho dt,$$

with a constant rate ρ, taking on values between -1 and 1. Within the scope of this model, we investigate various numerical methods for pricing European compound options.

A compound option is an option with another option as its underlying quantity. Due to this nested optionality, the compound option is characterized by two exercise decisions: the intermediate one of the 'mother option' and the final one of the 'daughter option'. When exercising the mother option the holder may decide to receive the underlying option for a fixed strike price paid in advance. That decision depends on the price of the daughter option at that future time and if the right to buy it for a fixed price is advantageous compared to the current market price of the underlying option. In turn, conditional on this prior decision, the second exercise is that of the underlying option at a later point in time. In the following we will deal with a standard compound call option, which is structured out of two European plain vanilla call options. Similarly, one can define a call on put, put on call, and put on put.

Suppose that a compound option expires at some future date T_M with the strike price K_M and the daughter option on which it is contingent, expires at a later time $T_D (> T_M)$ with the strike price K_D. Under geometric Brownian motion dynamics, the price of such a European call on a European call $M(S,t)$ (or call on call in short) at time t may be expressed as

$$M(S,t) = \mathbb{E}^{\mathbb{Q}}\left[e^{-r(T_M - t)}(D_{BS}(S_{T_M}, T_M) - K_M)^+ | S_t = S\right], \tag{3}$$

where $D_{BS}(S_{T_M}, T_M)$ is the Black-Scholes price of the underlying European call at time T_M when the underlying price is S_{T_M}. The exercise decision for D_{BS} depends on the future value of S_{T_D}. The operator $\mathbb{E}^{\mathbb{Q}}$ denotes the expectation operator under the risk neutral dynamics. Since the joint distribution of S_{T_M} and S_{T_D} in this model is well known, this expectation can be solved in terms of the univariate and bivariate normal cumulated distribution function and therefore can be calculated easily. The valuation of compound options in the Heston model poses a more difficult problem, since the exercise region of the mother option is multidimensional and also because the vanilla option pricing formula has a far more complicated format.

Under stochastic volatility dynamics, let $D(S, v, t)$ be the price of a European call option written on a stock of price S and given initial variance level v at time t with maturity time T_D and strike price K_D. Let $M(S, v, t)$ be the price of European call option written on the daughter option of price $D(S, v, t)$ with maturity time T_M and strike price K_M. Compared to the valuation of compound options in the Black-Scholes model, the uncertainty of volatility is incorporated into the dynamics of the Heston model and therefore into the price of the mother option as an additional risk factor of the market.

Now, the price M of a European compound option can be formulated as either the solution to a two-pass partial differential equation (PDE) problem or as the discounted expected payoff of the mother option. Both of the approaches relate to the use of conceptually different numerical methods to approximate the solutions. In the following sections, we first describe a selection of applicable methods and then we compare their performance.

3. Sparse Grid

In this section, we discuss a more general approach to price compound option prices using the sparse grid approach to solve the PDE satisfied by the prices of both daughter and mother options. Here, this approach is applied to price European compound options, but it can be easily generalized to handle compound options with early exercise or path dependent features.

Two-pass PDE formulation. We state the general two-step process below. First, we solve the PDE for the value of the daughter option $D(S, v, t)$ that satisfies:

$$\mathcal{K}D - rD + \frac{\partial D}{\partial t} = 0, \tag{4}$$

on the time interval $T_M \leq t \leq T_D$ and is subject to the terminal condition

$$D(S, v, T_D) = (S - K_D)^+. \tag{5}$$

Here, the Kolmogorov operator $\mathcal{K}$ is given by

$$\mathcal{K} = \frac{vS^2}{2}\frac{\partial^2}{\partial S^2} + \rho\sigma v S\frac{\partial^2}{\partial S \partial v} + \frac{\sigma^2 v}{2}\frac{\partial^2}{\partial v^2} + (r-q)\,S\frac{\partial}{\partial S} + (\kappa(\theta - v) - \lambda v)\frac{\partial}{\partial v}. \quad (6)$$

Next, we solve the PDE for the mother option $M(S, v, t)$ that satisfies:

$$\mathcal{K}M - rM + \frac{\partial M}{\partial t} = 0, \quad (7)$$

on the interval $0 \le t \le T_M$ and is subject to the terminal condition

$$M(S, v, T_M) = (D(S_{T_M}, v_{T_M}, T_M) - K_M)^+. \quad (8)$$

The prices of the daughter option are available from the solution of the PDE (4) with condition (5) and suitable boundary conditions as outlined below.

It seems computationally demanding to solve the two nested PDEs, however, we have applied a sparse grid approach to solve the PDEs in a fast and accurate manner. The sparse grid *combination technique* to solve PDEs was first introduced by Reisinger (2004) in his PhD thesis. Reisinger & Wittum (2007) discussed the application of this practically very attractive approach to option pricing problems. The combination technique only requires the solution of the original equation on conventional subspaces that are defined on Cartesian grids and a subsequent extrapolation step. But it is nevertheless able to retain a certain order of convergence due to the combination technique.

In the following, we outline the sparse grid approach to solve the PDEs (4) and (7) with suitable initial and boundary conditions.

Sparse Grid Implementation. In our case, we consider the two-dimensional cube $\Omega := [0, S_{\max}] \times [0, v_{\max}]$ and a Cartesian grid with mesh size $h_j = 2^{-l_j}$ (corresponding to a level $l_j \in \mathbb{N}_0$) for $j = 1, 2$. The indices $j = 1$ and $j = 2$ represent the directions of the stock price S and the variance v, respectively. For a vector $\mathbf{h} = (h_1, h_2)$, we define a grid with points

$$\mathbf{x}_h = (i_1 \cdot h_1,\ i_2 \cdot h_2) \quad \text{for} \quad 0 \le i_j \le N_j, \quad N_j = 2^{l_j}, \quad j = 1, 2.$$

For a given level l, the above grid consists out of all possible combinations of (l_1, l_2) with $0 \le l_1, l_2 \le l$. In total, there are $2^{2(l+1)}$ points in the grid. The curse of dimensionality come into effect as the level l increases. However, for a given level l, the sparse grid includes the following points

$$\mathbf{x}_h = (i_1 \cdot h_1,\ i_2 \cdot h_2) \quad \text{for} \quad 0 \le i_j \le N_j, \quad N_j = 2^{l_j}, \quad l_1 + l_2 = l, \quad j = 1, 2.$$

It is clear that there are $l+1$ choices of combinations of (l_1, l_2) which are: $(0,l),(1,l-1),\cdots,(l-1,1),(l,0)$. Figure 1 provides an example of a standard sparse grid with level $l=5$ with respect to different combinations:

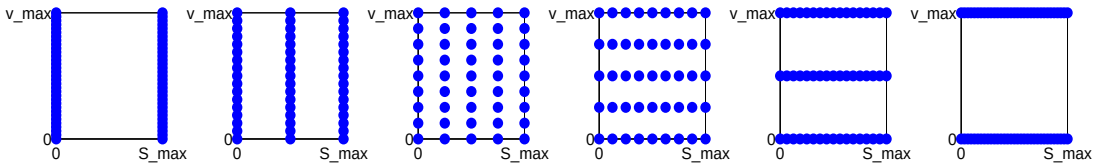

FIGURE 1. A sparse grid with a level 5 with respect to each combination. From the left to right, they are $(0,5),(1,4),(2,3),(3,2),(4,1),(5,0)$ respectively

Obviously, the above grids share the common property that they are dense in one direction, but sparse in the other direction. If we combine all of the above grids, we obtain the grid shown in Figure 2.

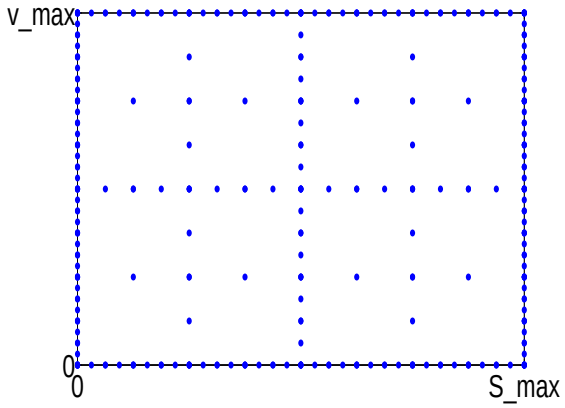

FIGURE 2. A standard sparse grid with a level 5.

Now, let $\mathbf{c}_h$ be the discrete vector of function values evaluated at the grid points. In general, $\mathbf{c}_h$ is the finite difference solution to the PDE of interest on the corresponding grid x_h. The solution can be extended to Ω by a suitable interpolation operator $\mathcal{I}$ in the pointwise sense according to

$$c_{\mathbf{h}}(S,v,\tau) = \mathcal{I}\mathbf{c}_h, \forall (S,v) \in \Omega.$$

Next, we define the family C of solutions corresponding to different grids (see Figure 1) by $C = (C(\mathbf{i}))_{\mathbf{i}\in\mathbb{N}^2}$ with

$$C(\mathbf{i}) := c_{2^{-\mathbf{i}}}.$$

That is the family of numerical approximations (after proper interpolation) $c_{\mathbf{h}}$ on tensor product grids with $h_k = 2^{-i_k}$. For example, the solution on the first grid in Figure 1

would be $C(0,5), C(1,4)$ and so forth. The combination technique in Reisinger & Wittum (2007) tells us that the solution c_l (l is the level of the sparse grid) of a corresponding PDE in two dimensions is given by

$$c_l = \sum_{n=0}^{l} C(n, l-n) - \sum_{n=0}^{l-1} C(n, l-1-n). \tag{9}$$

Now, the procedure is to solve the PDE in parallel on each of the sparse grids for level l and level $l-1$, respectively. Figure 1 shows the case $l=5$ as an example. Thus, there are $(2l+1)$ PDE solvers running at the same time. We combine all solutions together using equation (9) to find a more accurate solution of the PDE. In the following, we develop this approach a bit further.

Modified Sparse Grid Implementation. For our model, the underlying share price has different scale characteristics compared with the levels of the volatility. Hence, it is difficult to implement the above described sparse grid combination technique shown in Figure 1 directly. In fact, we found that it produces rather poor results. Furthermore, it is not straightforward to specify correct boundary conditions for some "extreme" grids, e.g. the first $(0,5)$ and the last $(5,0)$ grid in Figure 1 that uses only two points in one of the dimensions. Therefore, we have modified the above approach slightly by adding a fixed number of points to both, the $S-$ and $v-$directions in each of the grids. That result is a relative "balance" in both directions and numerical experiments show that this modification produces more accurate and efficient results.

More specifically, for both directions we let the levels l_1 and l_2 start from a small but non zero value l_s. That means that the new modified levels $\hat{l}_1, \hat{l}_2$ are defined as follows:

$$\hat{l}_1 = l_1 + l_s \text{ and } \hat{l}_2 = l_2 + l_s, \quad \text{with } l_1 + l_2 = l,\ l_1, l_2 \in \mathbb{N}_0.$$

Then, in terms of the level originally defined, l, the total level of the modified sparse grid becomes $2l_s + l$. Hence, the modified sparse grid consists of the following points:

$$\hat{\mathbf{x}}_h = (i_1 \cdot \hat{h}_1, i_2 \cdot \hat{h}_2), \quad \text{for } \hat{N}_j = 1/\hat{h}_j = 2^{\hat{l}_j},\ j = 1, 2,$$

where $\hat{l}_1 = l_1 + l_s,\ \hat{l}_2 = l_2 + l_s,\ l_1 + l_2 = l$. Similarly, there are still $l+1$ choices of combinations of (l_1, l_2): $(0,l), (1,l-1), \cdots, (l-1,1), (l,0)$. Consequently, we now have the levels $(l_s, l+l_s), (l_s+1, l+l_s-1), \cdots, (l_s+l-1, l_s-1), (l_s+l, l_s)$ for the modified sparse grid. Figure 3 provides an example of a modified sparse grid with $l_s = 2, l = 2$ $(2l_s + l = 6)$, namely $(2,4), (3,3), (4,2)$ as shown in Figure 4.

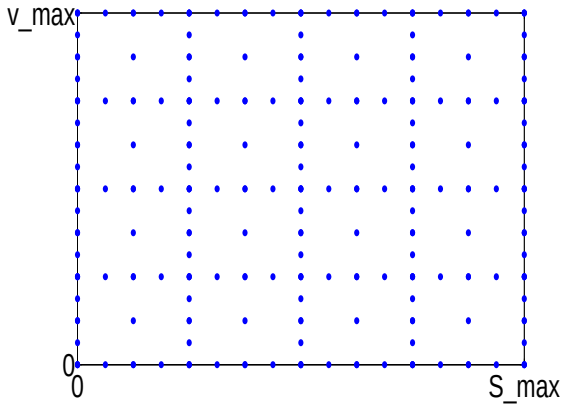

FIGURE 3. A modified sparse grid with a initial level 2 and total level 6.

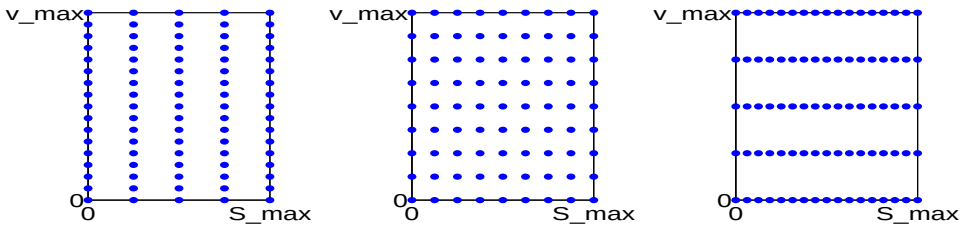

FIGURE 4. A modified sparse grid with a initial level 2 and total level 6 with respect to each combination.

Let l_s denote the initial level and l the level of the sparse grid. Then, analogous to equation (9), a solution $\hat{c}_{l_s,l}$ of a corresponding PDE in two dimensions on the modified sparse grid is given by

$$\hat{c}_{(l_s,l)} = \sum_{n=0}^{l} C(l_s+n, l_s+l-n) - \sum_{n=0}^{l-1} C(l_s+n, l_s+l-1-n). \tag{10}$$

We implement our modified sparse grid combination technique to solve the PDE (4) to obtain the desired daughter option prices. We then have the terminal and boundary conditions for the mother option. Next, we apply this technique again to solve the PDE (7) to obtain the prices of the mother option. In fact, we solve the PDEs (4) and (7) in each of the subspaces on a parallel cluster, which makes the computational process very efficient.

In the implementation, a PSOR method has been applied to each of the modified sparse grids in Figure 4 to calculate the solution of both PDEs (4) and (7) on the grid points and at other points by interpolation which is explained in more detail below.

Boundary conditions. The boundary conditions for the mother option are quite similar to those for the daughter option, hence for brevity, we only mention the boundary conditions for the daughter option here. For our subsequent discussion, let us denote the daughter option prices on an equidistant grid by

$$D^l_{i,j} = D(S_i, v_j, \tau_l), \quad \text{for } 1 \leq i \leq N_1 + 1,\ 1 \leq j \leq N_2 + 1,\ 1 \leq l \leq N_\tau,$$

where N_1, N_2 and N_τ are the number of grid points in the direction of S, v and τ, respectively. To this end, it is convenient to consider the time-to-maturity $\tau = T - t$ instead of time t.

Similar to the discussion in Ekstrom, Lotstedt & Tysk (2009), we use central differences to approximate most of the first and second derivatives in the PDE, but use the forward and backward finite difference approximations on the boundaries other than the time derivative in equation (4). Hence, we set

$$\frac{\partial D}{\partial S} = \frac{D^l_{i+1,j} - D^l_{i-1,j}}{2\Delta S},\ \frac{\partial^2 D}{\partial S^2} = \frac{D^l_{i+1,j} - 2D^l_{i,j} + D^l_{i-1,j}}{\Delta S^2},$$
$$\frac{\partial D}{\partial v} = \frac{D^l_{i,j+1} - D^l_{i,j-1}}{2\Delta v},\ \frac{\partial^2 D}{\partial v^2} = \frac{D^l_{i,j+1} - 2D^l_{i,j} + D^l_{i,j-1}}{\Delta v^2},$$

and

$$\frac{\partial D}{\partial S}|_{S=S_1} = \frac{D^l_{1,j} - D^l_{0,j}}{\Delta S},\ \frac{\partial D}{\partial S}|_{S=S_{N_1}} = \frac{D^l_{N_1,j} - D^l_{N_1-1,j}}{\Delta S},$$
$$\frac{\partial D}{\partial S}|_{v=v_1} = \frac{D^l_{i,1} - D^l_{i,0}}{\Delta v},\ \frac{\partial D}{\partial S}|_{v=v_{N_2}} = \frac{D^l_{i,N_2} - D^l_{i,N_2-1}}{\Delta v},$$

At $v = 0$, we fit a quadratic polynomial through the option prices at v_2, v_3 and v_4 which are the points closest to 0. Then, we employ the polynomial to extrapolate and to obtain an approximation of the price at $v = 0$. Additionally, we use the boundary condition $\frac{\partial^2 D}{\partial v^2} = 0$ at the boundary $v = v_{\max}$. The discretized analogues for all i, $i = 1, \ldots, N_1 + 1$, are

$$D^l_{i,N_2+1} = 2 \cdot D^l_{i,N_2} - D^l_{i,N_2-1},$$

which is essentially an extrapolation scheme. All other derivative terms in the $v-$direction vanish at $v = 0$ due to the factor v occurring in equation (4). That is why, these terms do not require further treatment.

We follow Ikonen & Toivanen (2007) to indicate which grid point values we use in order to obtain non positive off-diagonal weights in the finite difference stencil, which makes the matrix an $M-$matrix[1] as much as possible. In fact, to simplify the algorithm and to take consideration of the correlations ρ_{ij}, in each two dimensional space, we use a

[1]An $M-$matrix is a diagonally dominant matrix

seven point stencil. The mixed derivative is approximated as

$$\frac{\partial D^2}{\partial S \partial v} \approx \frac{1}{2}\left(\frac{D^l_{i+1,j+1} - D^l_{i,j+1} - D^l_{i+1,j} + D^l_{i,j}}{\Delta S \Delta v} + \frac{D^l_{i,j} - D^l_{i-1,j} - D^l_{i,j-1} + D^l_{i-1,j-1}}{\Delta S \Delta v}\right)$$

if $\rho_{12} > 0$ and as

$$\frac{\partial D^2}{\partial S \partial v} \approx \frac{1}{2}\left(\frac{D^l_{i,j+1} - D^l_{i-1,j+1} - D^l_{i,j} + D^l_{i-1,j}}{\Delta S \Delta v} + \frac{D^l_{i+1,j} - D^l_{i,j} - D^l_{i+1,j-1} + D^l_{i,j-1}}{\Delta S \Delta v}\right)$$

if $\rho_{12} < 0$.

The boundary conditions at the boundaries $S = 0$ and $S = S_{\max}$ for a call option are

$$D^l_{1,j} = 0 \text{ and } D^l_{N_1+1,j} = S_{\max} - K_D \cdot e^{-r \cdot \tau_l}, \quad \text{for } j = 1, \ldots, N_2 + 1,$$

while those for a put option are given by the discounted strike price of the daughter option.

The spatial discretization above leads to a semi-discrete equation which has the matrix representation

$$\frac{\partial \boldsymbol{D}}{\partial \tau} + \boldsymbol{A}\boldsymbol{D} = 0, \tag{11}$$

where $\boldsymbol{A}$ is a block tridiagonal $(N_1 + 1)(N_2 + 1) \times (N_1 + 1)(N_2 + 1)$ matrix and $\boldsymbol{D}$ is a vector of length $(N_1 + 1)(N_2 + 1)$. Next, we implement a more general $\theta-$scheme which includes the implicit Euler($\theta = 1$), the Crank-Nicolson ($\theta = \frac{1}{2}$) and the explicit Euler($\theta = 0$) scheme to discretize the semi-discrete problem (11) as

$$(\boldsymbol{I} + \theta \Delta \tau \boldsymbol{A})\, \boldsymbol{D}^{(l+1)} = (\boldsymbol{I} - (1-\theta)\Delta \tau \boldsymbol{A})\, \boldsymbol{D}^{(l)}, \quad \text{for } l = 0, \ldots, N_\tau - 1,$$

where $\boldsymbol{I}$ is the identity matrix.

After the discretization of the underlying PDE with two spatial variables an approximate price of a European option can be obtained by solving a sequence of linear systems as the one above. The initial value $\boldsymbol{D}^{(0)}$ is given by the discrete form of the payoff function of the option, so that the ith element of $\boldsymbol{D}^{(0)}$ is given by

$$\boldsymbol{D}^{(0)}_i = \max(S_i - K, 0).$$

In order to avoid the oscillations that often occur with the Crank-Nicolson scheme, we use the implicit Euler scheme for the first three time steps and then switch to the Crank-Nicolson scheme for the remaining time steps.

4. FFT Approach

Similarly to the valuation of compound options in the Black-Scholes model given in equation (3), the value of a compound option in the Heston model can be expressed as the discounted expected payoff under the risk-neutral measure $\mathbb{Q}_N$ (chosen by calibration to market data[2]) at the compound exercise date T_M. For example, a European compound call option with exercise times T_M and T_D with $0 < T_M < T_D$ and strike prices K_M and K_D at a time $t = 0$ is equal to

$$M(S_0, v_0) \quad = \quad e^{-rT_M}\mathbb{E}^{\mathbb{Q}_N}\left[(D(S_{T_M}, v_{T_M}) - K_M)^+\right],$$

where $D(S_{T_M}, v_{T_M})$ is the Heston model price of the underlying daughter European call at the exercise time of the compound option. Subsequently, we derive an expression for the compound call option that has a similar structure to the well-known compound option formula in the Black-Scholes model. With the help of indicator functions and a measure change[3], we can rewrite the above expression as the difference of three expectations

$$\begin{aligned} M(S_0, 0) \quad = \quad & e^{-qT_D} S_0 \underbrace{\mathbb{E}^{\mathbb{Q}_S}\left[\mathbb{1}_{\{D(S_{T_M}, v_{T_M}) \geq K_M\}} \mathbb{1}_{\{S_{T_D} \geq K_D\}}\right]}_{I} \\ & - e^{-rT_D} K_D \underbrace{\mathbb{E}^{\mathbb{Q}_N}\left[\mathbb{1}_{\{D(S_{T_M}, v_{T_M}) \geq K_M\}} \mathbb{1}_{\{S_{T_D} \geq K_D\}}\right]}_{II} \\ & - e^{-rT_M} K_M \underbrace{\mathbb{E}^{\mathbb{Q}_N}\left[\mathbb{1}_{\{D(S_{T_M}, v_{T_M}) \geq K_M\}}\right]}_{III}. \end{aligned} \tag{12}$$

The terms I, II and III are the exercise probabilities under the measures $\mathbb{Q}_S$ and $\mathbb{Q}_N$ of the daughter and mother options, respectively. In the Black-Scholes model these expectations can be resolved and are given by the normal distribution function in one and two dimensions as shown in Geske (1979). In the Heston model, the problem of solving these expectations is more complex, since it involves an additional dimension of uncertainty - the level of volatility at the exercise time of the mother option. In the following, we summarize the numerical pricing method for European compound options under the Heston model as developed in Griebsch (2012). This approach is based on a technique introduced by Dempster & Hong (2002) for pricing spread options. First, we

[2]To this end, we assume that the market price of volatility risk is equal to zero, $\lambda = 0$, without loss of generality.

[3]Choosing the stock price as numéraire, we switch from the risk-neutral measure to the measure $\mathbb{Q}_S$ according to the Radon-Nikodym derivative g_S defined by

$$g_S(T_D) \quad = \quad \exp\left(-(r-q)T_D + \ln S_{T_D} - \ln S_0\right) = \frac{d\mathbb{Q}_S}{d\mathbb{Q}_N}.$$

examine the third exercise probability III. The other two probabilities I and II can be computed in a similar way.

Approximation of the third exercise probability. Transferring the pricing problem into logarithmic space and setting $x_t = \ln S_t$ for all t, the term III yields

$$\begin{aligned}\mathbb{E}^{\mathbb{Q}_N}\left[\mathbb{1}_{\{D(x_{T_M},v_{T_M})\geq K_M\}}\right] &= \mathbb{P}^{\mathbb{Q}_N}\left(D(x_{T_M},v_{T_M})\geq K_M\right)\\ &= \iint_{E_M} f(v,x)dvdx,\end{aligned}$$

where f denotes the joint density with respect to volatility and logarithmic spot value at exercise time T_M. The integration region E_M represents the exercise region of the mother option and is given by

$$E_M = \left\{(x,v)\in\mathbb{R}^2_+ | D(x,v)\geq K_M\right\}.$$

Now, this exercise probability III is approximated by a Riemann sum of piecewise exercise probabilities as outlined subsequently. We use the grid structure which is induced by a fast Fourier transform method to construct an approximate integration region with $\tilde{E}_M \subset E_M$. Therefore, we take an equally spaced grid $\{x_0, x_1, \ldots, x_{N-1}\} \times \{v_0, v_1, \ldots, v_{N-1}\}$ on the scales of logarithmic spot values and volatility with fineness λ_x and λ_v, respectively, and approximate the continuous exercise region by

$$\begin{aligned}\tilde{E}_M &= \bigcup_{p=0}^{N-1} \tilde{E}_M(x_p, x_{p+1})\\ &= \bigcup_{p=0}^{N-1}\Big\{(x,v)\in\mathbb{R}^2_+\Big| x\in[x_p,x_{p+1}) \quad\wedge\quad \exists j\Big(v\geq v_j\wedge\forall x\in[x_p,x_{p+1})\\ &\qquad \{D(x,v_j)\geq K_M \quad\wedge\quad D(x,v_{j-1})<K_M\}\Big)\Big\}.\end{aligned}$$

Then, the approximation of term III can be expressed as a sum of double integrals

$$\iint_{E_M} f(v,x)dv\,dx \approx \iint_{\tilde{E}_M} f(v,x)dv\,dx = \sum_{p=0}^{N-1}\iint_{\tilde{E}_M(x_p,x_{p+1})} f(v,x)dv\,dx.$$

Using the notation

$$\mathbb{P}(x_p,\tilde{v}(x_p)) = \iint_{\tilde{E}_M(x_p,\infty)} f(v,x)dv\,dx \tag{13}$$

for the bivariate probabilities $\mathbb{P}(x_{T_M} \geq x_p, v_{T_M} \geq \tilde{v}(x_p))$ yields[4]

$$III \approx \sum_{p=0}^{N-2} \Big[\mathbb{P}(x_p, \tilde{v}(x_p)) - \mathbb{P}(x_{p+1}, \tilde{v}(x_p))\Big] + \mathbb{P}(x_{N-1}, \tilde{v}(x_{N-1})).$$

Application of FRFT. To compute a set of such bivariate probabilities $\mathbb{P}(x, \tilde{v})$, we use the one-dimensional fractional fast Fourier transform (FRFT) method, which was first introduced in the context of option pricing by Chourdakis (2005). Therefore, we employ the well-known technique developed in Carr & Madan (1999) and express the dampened probability (by using parameters $\alpha > 0$ and $\beta > 0$) as the inverse Fourier transform of χ given by:

$$e^{\alpha x_p + \beta \tilde{v}_p} \mathbb{P}(x_p, \tilde{v}_p) = \frac{1}{(2\pi)^2} \iint_{\mathbb{R}^2} e^{-iw_x x_p - iw_v \tilde{v}_p} \chi(w_x, w_v) dw_v dw_x, \tag{14}$$

where χ in turn is the Fourier transform of the dampened probability $\mathbb{P}(\cdot, \cdot)$. But contrary to the probability $\mathbb{P}(\cdot, \cdot)$, the function χ can be expressed in closed-form via the characteristic function φ of x_{T_M} and v_{T_M} as

$$\chi(w_x, w_v) = \frac{\varphi_{x,v}(w_x - i\alpha, w_v - i\beta)}{(\alpha + iw_x)(\beta + iw_v)}.$$

where the definition of $\varphi_{x,v}$ is given in the appendix. Moreover, the inverse Fourier transform of χ with respect to volatility can be solved. Hence, equation (14) becomes

$$\mathbb{P}(x_p, \tilde{v}_p) = \frac{1}{2\pi} e^{-\alpha x_p} \int_{-\infty}^{\infty} e^{-iw_x x_p} \frac{1}{\alpha + iw_x} g(w_x - i\alpha, \tilde{v}_p) dw_x. \tag{15}$$

The function g is defined as

$$\begin{aligned} g(\bar{w}_x, \tilde{v}_p) = {} & \exp\left(i\bar{w}_x x_0 + i\bar{w}_x (r-q) T_M - i\bar{w}_x \frac{\rho}{\sigma}(v_0 - \kappa\theta T_M) + \frac{\kappa\theta}{\sigma^2}(\kappa - d) T_M\right) \\ & \times \exp\left(-\frac{(de^+ - \kappa e^-)}{\sigma^2 e^-} v_0\right) m^{-\frac{2\kappa\theta}{\sigma^2}} F_{\chi'^2_{df}(c)}\left(\frac{4dm}{\sigma^2 e^-} \tilde{v}_p\right) + R, \end{aligned}$$

where $e^{\pm} = 1 \pm \exp(-dT_M)$ and

$$\begin{aligned} d &= \sqrt{\kappa^2 + 2\sigma^2\left(\frac{1}{2} i\bar{w}_x - \kappa\frac{\rho}{\sigma} i\bar{w}_x + \frac{1}{2}\bar{w}_x^2(1-\rho^2)\right)}, \\ m &= \frac{de^+ + \kappa e^- - i\bar{w}_x \rho\sigma e^-}{2d}. \end{aligned}$$

The term R denotes the residue of the function g. The function F denotes the cumulative distribution function for non-central chi-squared random variables with the number of degrees of freedom equal to $\frac{4\kappa\theta}{\sigma^2} = df$, a non-centrality parameter $c = \frac{4de^{-d\tau}}{\sigma^2 e^- m} v_0$ and

[4]The function $\tilde{v} : \mathbb{R} \to \{v_0, v_1, \ldots, v_{N-1}\}$ is implicitly given by the definition in (13).

complex arguments.

As a consequence, the probabilities in (15) can now be approximated by

$$\mathbb{P}(x_p, \tilde{v}_p) \approx \frac{e^{-\alpha x_p}}{2\pi}\delta_x e^{\frac{1}{2}iN\delta_x\lambda_x p}\sum_{m=0}^{N-1} e^{-i\lambda_x\delta_x mp}\left[\frac{e^{-iw_{x,m}x_0}}{\alpha+iw_{x,m}}\mu_m g(w_{x,m}-i\alpha,\tilde{v}_p)\right], \quad (16)$$

where δ_x determines the accuracy of the integral approximation and λ_x controls the quality of approximation of the exercise region. The variable w_x of the Fourier transform on the discrete FFT grid is denoted by $w_{x,m}$ and is determined by the choice of δ_x. The format of the quantities μ_m, for all m, depends on the choice of the integral approximation scheme (e.g. the trapezoidal rule).

To conclude, by setting the input parameters of the one-dimensional FRFT routine with values as given in the squared brackets in the expression above, the output array contains approximation values of $\mathbb{P}(x_p, \tilde{v}_p)$ for all x_p with the same level of volatility $\tilde{v}_p$, which are used to approximate the exercise probability III.

Approximation of the other two exercise probabilities. In the same manner, the exercise probabilities I and II are approximated by using an approximate exercise region of the daughter option E_D as

$$\tilde{E}_D = \tilde{E}_M \times \{x_{T_D} \geq k_D\},$$

with $k_D = \log(K_D)$. The trivariate density of x_{T_D}, x_{T_M} and v_{T_M} is denoted by $f^{\mathbb{Q}_S}$ or $f^{\mathbb{Q}_N}$ and the exercise probability of the daughter option under the corresponding measures $\mathbb{Q}_N$ and $\mathbb{Q}_S$, is approximated by

$$\begin{aligned} I &= \int_{k_D}^{\infty}\iint_{E_M} f^{\mathbb{Q}_S}(v, x_M, x_D)dvdx_M dx_D \\ &\approx \sum_{p=0}^{N-2}\left[\mathbb{P}^{\mathbb{Q}_S}(x_p,\tilde{v}_p,k_D) - \mathbb{P}^{\mathbb{Q}_S}(x_{p+1},\tilde{v}_p,k_D)\right] + \mathbb{P}^{\mathbb{Q}_S}(x_{N-1},\tilde{v}_{N-1},k_D). \end{aligned}$$

and

$$\begin{aligned} II &= \int_{k_D}^{\infty}\iint_{E_M} f^{\mathbb{Q}_N}(v, x_M, x_D)dvdx_M dx_D \\ &\approx \sum_{p=0}^{N-2}\left[\mathbb{P}^{\mathbb{Q}_N}(x_p,\tilde{v}_p,k_D) - \mathbb{P}^{\mathbb{Q}_N}(x_{p+1},\tilde{v}_p,k_D)\right] + \mathbb{P}^{\mathbb{Q}_N}(x_{N-1},\tilde{v}_{N-1},k_D). \end{aligned}$$

In the formula above, we used a short notation for the trivariate probabilities $\mathbb{P}(x_{T_M} \geq x_p, v_{T_M} \geq \tilde{v}_p, x_{T_D} \geq k_D)$ in the same sense as for the bivariate case in equation (13). Note that, the exercise region with respect to x_{T_D} is linear. Similar to the case of

expectation III, we employ the approach of Carr & Madan: we dampen $\mathbb{P}(\cdot,\cdot,\cdot)$ using constants $\alpha,\beta,\gamma>0$, and identify its Fourier transform χ as a closed-form expression of the characteristic function of $(v_{T_M}, x_{T_M}, x_{T_D})$. Then in turn, the inverse Fourier transform of χ gives us an expression for $\mathbb{P}(\cdot,\cdot,\cdot)$ in terms of the trivariate characteristic function. Furthermore, the integration with respect to the volatility dimension can be resolved under each measure $\mathbb{Q}_N$ and $\mathbb{Q}_S$. Let this solution be denoted by the function[5] h. Therefore, for all $p,q=0,\ldots,N-1$, every trivariate probability can be reduced to a double integral

$$\begin{aligned}\mathbb{P}(x_p^M,\tilde{v}_p,x_q^D) &= \frac{e^{-\alpha x_p^M-\gamma x_q^D}}{(2\pi)^2}\iint_{\mathbb{R}^2} e^{-iw_{x_M}x_p^M-iw_{x_D}x_q^D}\\ &\quad\times\frac{h(w_{x_M}-i\alpha,\tilde{v}_p,w_{x_D}-i\gamma)}{(\alpha+iw_{x_M})(\gamma+iw_{x_D})}dw_{x_M}\,dw_{x_D}.\end{aligned}$$

The quantities x_p^M and x_q^D take values on a two-dimensional FFT grid on $\mathbb{R}_+^2$ with a fineness of λ_x and a starting value x_0. The scale of the volatility values can be chosen independently of an FFT grid. Finally, the probabilities can be approximated by double sums of the form

$$\begin{aligned}\mathbb{P}(x_p^M,\tilde{v}_p,x_q^D) &\approx \frac{e^{-\alpha x_p^M-\gamma x_q^D}}{(2\pi)^2}\delta_x^2 e^{\frac{1}{2}iN\lambda_x\delta_x(p+q)}\sum_{n=0}^{N-1}\sum_{m=0}^{N-1}e^{-i\lambda_x\delta_x(mp+nq)}\\ &\quad\times\left[\mu_{m,n}\frac{e^{-ix_0(w_{M,m}+w_{D,n})}h(w_{M,m}-i\alpha,\tilde{v}_p,w_{D,n}-i\gamma)}{(\alpha+iw_{M,m})(\gamma+iw_{D,n})}\right],\end{aligned}\tag{17}$$

where δ_x controls the discretization error of the approximation and $\mu_{m,n}$ define the weights of the 2D trapezoidal rule. As shown in Griebsch (2012), for parameters $\eta_1=\frac{\lambda_x\delta_x}{2\pi}$ and $\eta_2=0$ the two-dimensional discrete FRFT computes sums of the format in equation (17) above using three calls of two-dimensional FFTs. In contrast to using the standard FFT algorithm, the application of the fractional FFT allows us to choose λ_x and δ_x independently from each other.

The method outlined above, describes how to compute lower bounds for all three exercise probabilities of equation (12). Equivalently, one derives formulas for computing upper bounds of I, II and III. The average of these computing results for each probability together with representation (12) provides us with an approximation for a European compound call option price under Heston model dynamics.

Remarks on the implementation. Note that, the infinite integration domain $(-\infty,\infty)$ of the integral in (15) is approximated by a finite integration domain thereby

[5]The definition is given in the appendix.

introducing a truncation error. Also, the domain of the Fourier variable w_x is discretized and a suitable quadrature rule is applied, which leads to a discretization error. To reduce the error introduced by these two types of approximations and therefore to improve the accuracy of the method, one possibility is to make use of the symmetric properties of the characteristic function and to express the integral in (15) on the positive real line $\mathbb{R}_+$ only (and respectively, the double integrals in (17) on the positive real quadrant $\mathbb{R}_+^2$).

To further improve the pricing technique in regard to the computational runtime, we choose the number of grid points and the fineness of the grid with respect to volatility independently of the FRFT algorithm. This is possible due to the dimension reduction of the integral in (14) by solving the inverse Fourier inversion with respect to volatility (given in function g). Additionally, the set of volatility values $\{v_0, v_1, \ldots, v_{M-1}\}$ can be chosen to be equidistant or according to the non-central chi-squared distribution, for instance, so that a higher number of bivariate probabilities $\mathbb{P}(x_{T_M} \geq x_p, v_{T_M} \geq \tilde{v}(x_p))$ contribute to the approximation of the exercise probabilities in regions where the density of the volatility places more weight.

Moreover, we store all results for probabilities $\mathbb{P}(x_{T_M} \geq x_p, v_{T_M} \geq \tilde{v}(x_p))$, for $p = 0, \ldots, N-1$, for which the level of volatility $\tilde{v}(x_p)$ in the computation of upper and lower bounds is the same. Hence, the number of calls to the FRFT routine is governed by the slope of the boundary of the exercise region E_M (and E_D, respectively) and the denseness of the discrete grid in areas of the exercise region with steep descending boundaries. For example, for high initial spot values the compound option is always exercised at T_M, irrespective of how low the initial volatility level is, which implies that the boundary of the exercise region has slope equal to zero and only one FRFT call needs to be made in order to compute all bivariate probabilities for this area. In the same manner, the probabilities used to approximate the upper bounds of the exercise probabilities I, II and III are reused for the approximation of the corresponding lower bounds.

5. Transition Density Approach

An alternative method to compute compound option prices in the Heston model is to use the knowledge of the Green's function for spot and volatility values, which is described in this section.

In Chiarella, Ziogas & Ziveyi (2010), the authors show that in the Heston model every European option whose payoff at a future time t depends on the volatility and spot value

can be expressed at time 0 as

$$\text{European option price} \;=\; e^{-rt}\int_0^\infty\int_{-\infty}^\infty \text{payoff}(v_t,x_t)\,G(x_t,v_t,t;x_0,v_0)\,dx_t\,dv_t,$$

for given starting values $x_0 = \log(S_0)$ and v_0. The Green's function G is given by the bivariate inverse Fourier transform of the bivariate characteristic function $\varphi_{x,v}$ of logarithmic spot and volatility as

$$\begin{aligned} G(y,w,t;x_0,v_0) \;=\; & \frac{1}{2\pi}\int_{-\infty}^\infty e^{iuy}e^{-iux_0-iu(r-q)\tau}e^{\frac{\kappa+\rho\sigma iu-d}{\sigma^2}(v_0-w+\kappa\theta\tau)} \\ & \times e^{\frac{-2d}{\sigma^2(e^{dt}-1)}(we^{dt}+t)}\frac{2de^{dt}}{\sigma^2(e^{dt}-1)}\left(\frac{we^{dt}}{v_0}\right)^{\frac{\kappa\theta}{\sigma^2}-\frac{1}{2}} \\ & \times I_{\frac{2\kappa\theta}{\sigma^2}-1}\left(\frac{4d}{\sigma^2(e^{dt}-1)}\sqrt{wv_0e^{dt}}\right)du \end{aligned}$$

with $d = \sqrt{\kappa+\rho\sigma iu-\sigma^2(iu-u^2)}$ and $I_{\frac{2\kappa\theta}{\sigma^2}-1}$ is modified Bessel function of the first kind of the order indicated.

Therefore, the compound option pricing problem in the Heston model can be stated with respect to the transition density as

$$\begin{aligned} M(S_0,v_0) \;&=\; e^{-rT_M}\mathbb{E}^{\mathbb{Q}_N}\left[(D(S_{T_M},v_{T_M})-K_M)^+\right] \\ &=\; e^{-rT_M}\int_{\mathbb{R}}\int_{\mathbb{R}_0^+}(D(\exp(y),w)-K_M)^+\,G(y,w,T_M;x_0,v_0)dwdy. \end{aligned}$$

The above representation can be evaluated using numerical integration routines.

In Lipton (2001), section 13.11, a similar result for European weakly path-dependent options is obtained. It could also be applied in this case, although it involves a higher number of integrals to be numerically approximated. In addition, the knowledge of the transition density G could be combined with the FFT algorithm described above. That algorithm approximates the exercise probabilities by Riemann sums. Hence, the approximation of exercise probability III becomes more accurate the finer the grid for regions where the derivative of $G \times \mathbb{1}_{E_M}$ is large. An equivalent criterion can be formulated for the exercise probabilities I and II.

6. MC simulation

The implementation of a Monte Carlo simulation mainly serves the purpose of making the comparison between the other described numerical methods. We give a brief description of the Monte Carlo set-up we use here. In a first step, we run a Monte Carlo simulation for the underlying process and obtain in this way a number of spot prices and

variance values at the exercise time of the mother option. Next, based on this sample we compute the corresponding daughter option prices using the Fourier Cosine expansion (COS) by Fang & Oosterlee (2008).

We use Euler discretization together with the full truncation scheme introduced in Lord, Koekkoek & Dijk (2010) to approximate the paths of the underlying process and variance process on a discrete time grid. The full truncation scheme is designed to avoid negative values for the variance process. For this, the time interval for the mother option $[0, T_M]$ is partitioned into m equal segments of length $\Delta t = T_M/m$, i.e., $t_i = i\Delta t$ for $i = 0, 1, \ldots, m$.

(1) The discretization for the logarithmic spot price process is:

$$\begin{aligned} x_{t_i} &= x_{t_{i-1}} + \left(r - q - \frac{1}{2}\max\{v_{t_{i-1}}, 0\}\right)\Delta t \\ &\quad + \sqrt{\max\{v_{t_{i-1}}, 0\}}\left(\rho\Delta Z_{t_i}^{(1)} + (1-\rho^2)\Delta Z_{t_i}^{(2)}\right), \end{aligned} \tag{18}$$

where $\Delta Z_{t_i}^{(j)} = Z_{t_i}^{(j)} - Z_{t_{i-1}}^{(j)}$ for $j = 1, 2$.

(2) The discretization for the variance process is

$$v_{t_i} = v_{t_{i-1}} + \kappa(\theta - \max\{v_{t_{i-1}}, 0\})\Delta t + \sqrt{\max\{v_{t_{i-1}}, 0\}}\sigma\Delta Z_{t_i}^{(1)}. \tag{19}$$

To simulate the Brownian increments, the fact that each increment $Z_{t_i}^{(j)} - Z_{t_{i-1}}^{(j)}$ is independent of others is used. Each such increment is normally distributed with mean 0 and standard deviation $\sqrt{\Delta t}$.

Simulating N spot and variance process paths from time 0 up to time T_M according to equations (18) and (19) given the starting values x_0 and v_0, we obtain a sample of $S_{T_M}^{(k)}$ and $v_{T_M}^{(k)}$ for $k = 1, \ldots, N$. Hence, the expected payoff of the mother option is estimated by

$$M(S_0, v_0) = \frac{1}{N}\sum_{k=1}^{N}\max\{D\left(S_{T_M}^{(k)}, v_{T_M}^{(k)}\right) - K_M, 0\}, \tag{20}$$

where the price of the daughter option $D(S_{T_M}^{(k)}, v_{T_M}^{(k)})$ is available as a result of the COS method.

7. Numerical Analysis

In this section, we report on the performance of the four structurally different pricing methods for computing European compound options in the Heston model as outlined in the previous sections.

Method specifications. The methods are assessed using the following specifications:

The modified sparse grid method (SG) is tested for levels between 4 and 7 to compute prices for the mother option. To compute the price of the underlying daughter option at the exercise time T_M two approaches are compared - either using sparse grids once more or using the Fourier Cosine Expansion (COS) approach described in Fang & Oosterlee (2008) to work out the vanilla option prices in the Heston model. In the COS setting, $N = 256$ cosine terms are used with the truncation range calculated from the formulae in Fang & Oosterlee (2008).

The fractional fast Fourier transform approach (FRFT) is assessed for a different number of grid points ($N = 64, 128, 256, 512$) on the logarithmic spot scale. The number of grid points on the volatility scale can be chosen independently of N and is found to be sufficiently high for a choice of 100 points. First, the computations are carried out using an equidistant volatility grid and then compared to the results when generating a randomly sampled volatility grid. Before starting the compound option evaluation, the damping factor is chosen by running an optimization to minimize the difference between computing an arbitrarily chosen bivariate probability of the form $\mathbb{P}(x_{T_M} \geq x_p, v_{T_M} \geq \tilde{v}(x_p))$ in two ways: with the FRFT technique, as a function of α; then using numerical integration and the representation[6] as stated by Shephard (1991). This gives us a damping factor of approximately 1.75. The integration grid size is controlled by the domain of the function g, which can be found by applying a simple root search algorithm. The fineness of the two-dimensional grid for logarithmic spot and volatility values is determined by the support of the state space of the three random variables x_{T_M}, v_{T_M} and x_{T_D} and are therefore fixed as well. The weights μ_m in (16) and $\mu_{m,n}$ in (17) are set according to the trapezoidal rule.

Based on the discretization scheme in (18) and (19), we run Monte Carlo (MC) simulations to estimate the price of the mother option using 0.1 million, 0.5 million, 1 million and 5 million sample paths for logarithmic spot and volatility and 500 time steps. The random number generator provided by Matlab is used. Antithetic variates are applied to reduce the variance of the estimated expectation. As with the sparse grid approach, to compute the price of the underlying daughter option, the COS method is employed. This stabilizes the results compared to using Monte Carlo simulation for the mother as well as for the daughter option.

For the transition density, the Greens function approach, we use the adaptive Simpson quadrature routines, dblquad, provided by Matlab to numerically evaluate the double integral over the compound option payoff with respect to the Green's function. In a first

[6]In Shephard (1991), the author shows that a bivariate distribution function $F_{x_{T_M}, v_{T_M}}$ can be computed by computing the univariate distribution functions, $F_{x_{T_M}}$ and $F_{v_{T_M}}$, and a double integral with respect to the characteristic function of the corresponding random variables, x_{T_M} and v_{T_M}.

step, the default tolerance $1.0e^{-6}$ is left unchanged when measuring the computational runtime. In a later step, for the assessment of the relative mean squared error the tolerance is set to a lower level. The integration limits are from 0 to 1 for the volatility direction and to 10.0 for the integration with respect to the logarithmic spot price introducing the same level of truncation error as for the FRFT technique.

Model parameters. We test the numerical pricing methods for a number of different sets of Heston model parameters in order to compare their accuracy and computational times. The first two test cases, given in table 1, each define Heston model dynamics where the model parameters fulfill the Feller condition and where parameters are constant for the entire lifetime of the compound option. The model correlation is chosen to be positive in the first test case and negative for the second one. The third test case, given in table 4, represents a model parameter set which was obtained by calibration to market data and which allows for time-dependent (piecewise constant) parameters. Contrary to the first two test cases, this set does not fulfill the Feller condition, which is often found to be the case in practical applications of the Heston model.

Pricing results. Given the model parameter set in table 1 with positive correlation, we obtain the compound option prices in table 2 using the four above listed methods for initial spot prices ranging from 80 to 120. The source code for all methods was

Parameter	Value	SV Parameter	Value
r	0.03	θ	0.04
q	0.05	κ	2.00
T_D	1.0	σ	0.20
K_D	100	λ	0.00
T_M	0.60	ρ	± 0.50
K_M	7	v_0	0.04

TABLE 1. Parameter values used for the European compound call option. The stochastic volatility (SV) parameters correspond to the Heston model.

implemented using Matlab 2012a running on the UTS, Faculty of Business F&E HPC Linux Cluster which consists of 8 nodes running Red Hat Enterprise Linux 6.2 (64bit) with 2×3.33GHz 12MB Cache Intel Xeon 5680 (Six Core) Processors, 24GB DDR3-1333 ECC Memory (Triple Channel). Since the methods using sparse grid, fractional fast Fourier transform and Monte Carlo simulation are natural applications of parallel computing, we divide the computations for each method up into several smaller tasks and solve them concurrently. For the sparse grid method, the problem of computing

compound option prices can be divided into solving 13 partial differential equations concurrently for level 5, for instance. Sampling logarithmic spot and volatility paths in the Monte Carlo simulation we make use of the parfor-loop[7] with 12 CPU's for each initial spot value. For the fractional fast Fourier transform approach we distribute the computation of the bi - and trivariate probabilities, as given in the equations (16) and (17), on 12 CPU's using the parfor-loop. Then the computational runtime is determined by the node with the longest runtime. For each method it is reported in table 2.

Method			S			Runtime
	80	90	100	110	120	(sec)
COS + SG(4)	0.3112	1.1478	3.2054	7.1457	13.1982	51
COS + SG(5)	0.3085	1.1428	3.2057	7.1428	13.1787	141
COS + SG(6)	0.3085	1.1418	3.2066	7.1501	13.1837	536
COS + SG(7)	0.3090	1.1430	3.2087	7.1535	13.1860	3001
FRFT (64,100)	0.3093	1.1443	3.2133	7.1656	13.2113	51
FRFT (128,100)	0.3086	1.1421	3.2073	7.1516	13.1843	145
FRFT (256,100)	0.3088	1.1425	3.2080	7.1525	13.1851	1499
Green	0.3088	1.1427	3.2084	7.1530	13.1855	33-113
COS +MC(5M)	0.3081	1.1419	3.2075	7.1541	13.1876	3119
std err	0.0007	0.0014	0.0025	0.0037	0.0049	
Lower Bound	0.3066	1.1390	3.2026	7.1468	13.1780	
Upper Bound	0.3094	1.1447	3.2124	7.1614	13.1972	

TABLE 2. European Compound call prices computed using sparse grid (SG), fractional fast Fourier transform (FRFT) with $N = 64, 128, 256$ and $M = 100$, numerical integration of the Green's function (Green), Monte Carlo simulation (MC). Parameter values are given in Table 1, with $\rho = 0.50$.

For the given runtime, we note that the sparse grid method and Monte Carlo simulation is able to compute a range of compound option prices, whereas the runtime for the Green's function approach is for the specified compound option only. Hence, if only one compound option price needs to be evaluated, using the Green's function seems to be the fastest method. However, the runtime of Matlab's numerical integration varies, meaning that it increases for increasing initial spot level. This general observation can also be made when looking at table 3, which reports compound option prices for the case with negative model correlation. Overall, we observe a converging behavior of the sparse grid method and the fractional fast Fourier transform approach to the prices given by

[7]'Parfor' is a pMatlab command which allows us to write a loop for a statement or block of code that executes in parallel on a cluster of computers.

using the Green's function, which lie in the 95% - confidence intervals for the Monte Carlo simulation. Therefore, in a next step, we take the results of this approach with

Method			S			Runtime
	80	90	100	110	120	(sec)
COS + SG(4)	0.0693	0.6666	2.8055	7.2317	13.7291	51
COS + SG(5)	0.0645	0.6429	2.7805	7.2245	13.7274	138
COS + SG(6)	0.0686	0.6465	2.7877	7.2308	13.7287	539
COS + SG(7)	0.0683	0.6450	2.7874	7.2309	13.7288	2934
FRFT (64,100)	0.0684	0.6446	2.7911	7.2449	13.7574	50
FRFT (128,100)	0.0683	0.6441	2.7865	7.2302	13.7282	142
FRFT (256,100)	0.0684	0.6447	2.7875	7.2311	13.7288	1451
Green	0.0685	0.6450	2.7880	7.2315	13.7291	25 - 121
COS + MC (5M)	0.0686	0.6455	2.7885	7.2315	13.7296	2919
std err	0.0002	0.0008	0.0019	0.0031	0.0043	
Lower Bound	0.0681	0.6439	2.7849	7.2254	13.7213	
Upper Bound	0.0690	0.6471	2.7922	7.2376	13.7380	

TABLE 3. Compound prices (European call on European call) computed using sparse grid (SG), fractional fast Fourier transform (FRFT) with $N = 64, 128, 256$ and $M = 100$, numerical integration of the Green's function (Green), Monte Carlo simulation (MC) together with MOL. Parameter values are given in Table 1, with $\rho = -0.50$.

a tolerance level of 1.0×10^{-12} to be the true price and analyze the relative root mean squared error for all other methods.

Results for RMSE. In figures 5 and 6, we plot the relative root mean squared error (RMSE) against runtime on a logarithmic scale. The RMSE for the Monte Carlo simulation is shown as triangles, the errors for the sparse grid method as squares and those for the fractional fast Fourier transform as circles. The graph shows that the FRFT approach depends on the choice of the damping factor, which ensures the square-integrability of the inverse Fourier transform of χ with respect to the logarithmic spot price. We observe the effect on the convergence of the method when choosing different values for the damping factor α. The solid line gives the RSME for a lower damping factor, $\alpha = 1.0514$, and the dashed line for a higher damping factor, $\alpha = 1.75$. For the Monte Carlo simulations, there is a variety of results but they achieve a relative accuracy of at least up to 6.0×10^{-6} and 8.0×10^{-7} for each price with a standard deviation of at most 0.0014 and 0.0019 for the positive and negative correlation case, respectively. The sparse grid method combined with the COS method, shown as a solid

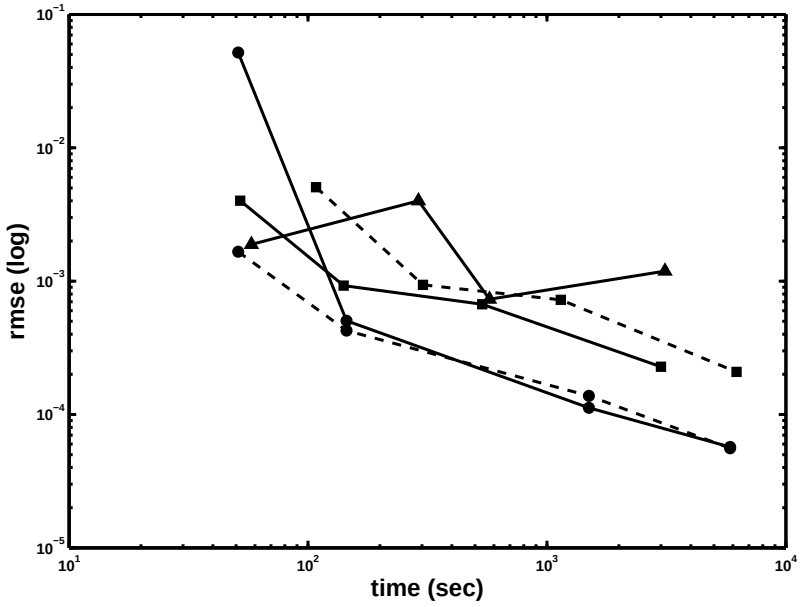

FIGURE 5. The figure shows the relative mean squared error on a logarithmic scale of the sparse grid (square), Monte Carlo simulation (triangle) and the FRFT approach (circle) to the results from the numerical integration of the Green's function. Parameter values are given in Table 1, with $\rho = 0.50$.

line, shows a normal convergence for both cases of a positive and a negative correlation. For level 7, it reaches a relative accuracy of at least 1.6×10^{-6} and 6.6×10^{-6} for the positive and negative correlation case, respectively. Using the sparse grid method on the prices computed with sparse grids, shown as a dashed line, yields less accurate results. The fractional fast Fourier transform technique shows the best convergence to the results obtained with using the Green's function in the test case with negative correlation, but for the positive correlation case, the choice of pricing method is not a clear cut decision and depends on the constraints on computational time. For $N = 512$ the FRFT approach reaches a relative accuracy of at least 1.7×10^{-7} for the negative correlation case and 1.1×10^{-8} for the positive correlation case for each compound option price.

Time-dependent parameters. The third model parameter set for which we studied the pricing of compound options was obtained by calibrating the Heston model with time-dependent (piecewise constant) model parameters with respect to the two periods $[0, T_M]$ and $[0, T_D]$ given the volatility smiles of the EURUSD on the 15th of May, 2012, as shown in figure 7.

All of the pricing methods were extended to allow for this piecewise constant, but time-dependent Heston model. The results in table 5 show the agreement of the methods

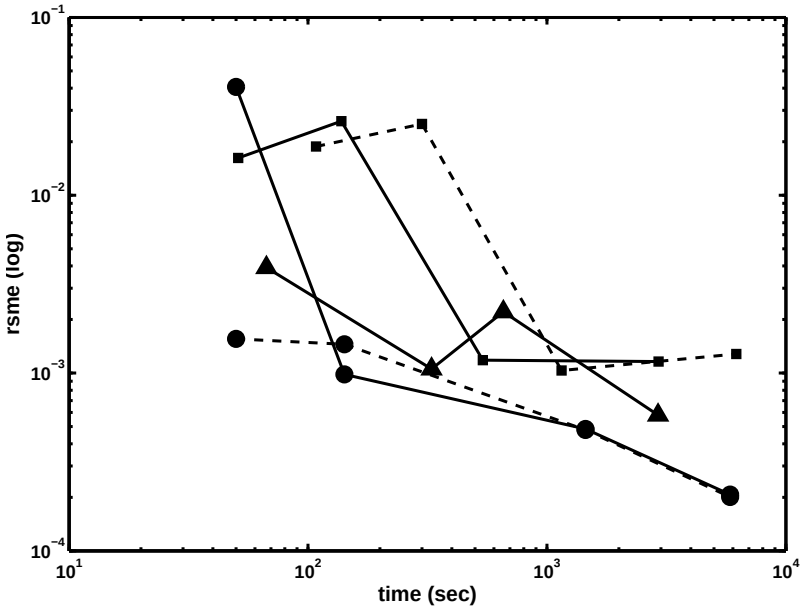

FIGURE 6. The figure shows the relative mean squared error on a logarithmic scale of the sparse grid (square), Monte Carlo simulation (triangle) and the FRFT approach (circle) to the results from the numerical integration of the Green's function. Parameter values are given in Table 1, with $\rho = -0.50$.

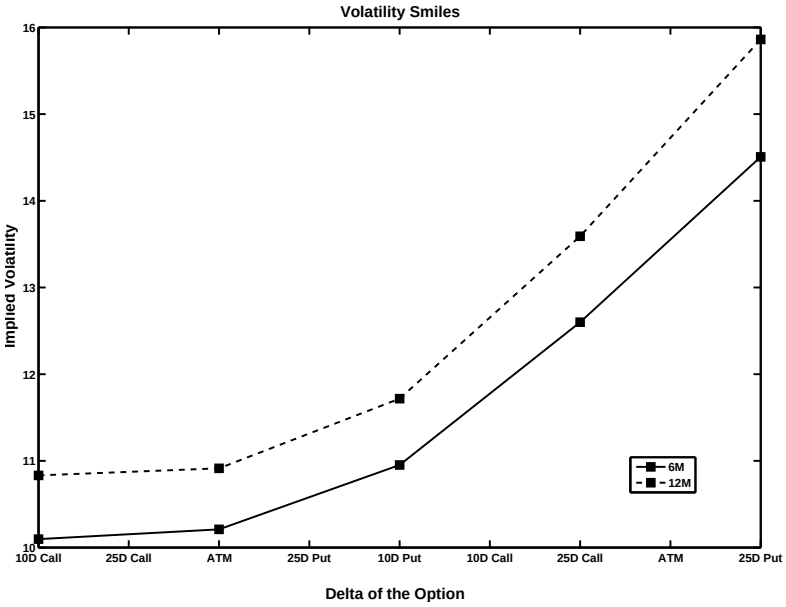

FIGURE 7. EURUSD Volatility smiles for 6 and 12 months. Date 15. May 2012.

even with time-dependent piecewise constant model parameters and the unmet Feller condition. The FRFT technique and the approach using the Green's function are applied

Parameter	Value	Parameter Set 1	Value	Parameter Set 2	Value
r_d	0.1550%	θ	0.0284	θ	0.0314
r_f	0.2442%	κ	3.7985	κ	2.4922
S_0	1.2729	σ	0.5792	σ	0.565
v_0	0.01	ρ	-0.5683	ρ	-0.5542
K_D	1.2729	λ	0.0	λ	0.0
K_M	0.068	T_M	0.50	T_D	1.0

TABLE 4. Parameter values used for the European compound call option. The stochastic volatility (SV) parameters correspond to the Heston model.

Method	Price
COS + SG(7)	0.024468
FRFT (128,100)	0.024422
Green	0.024436
MC (5Mio)	0.024412
95% confidence interval	(0.024327,0.024497)

TABLE 5. Compound prices (European call on European call) computed using sparse grid (SG), fractional fast Fourier transform (FRFT), numerical integration of the Green's function (Green), Monte Carlo simulation (MC). Parameter values are given in Table 4.

with integration limits of $[0, 1]$ and $[0, 0.25]$ for logarithmic spot and volatility values. For Matlab's dblquad routine a tolerance level of 1.0×10^{-9} is used. All methods agree up to the fourth digit and lie in the 95%-confidence interval of the Monte Carlo simulations. Note that, the runtimes of the methods using the Green's function and the FRFT can be further improved for the cases of Heston model parameters when $2\kappa\theta/\sigma^2 \in [0, 1]$. Then the density of v exhibits near-singular behavior. This behavior is described in Fang & Oosterlee (2011) and a logarithmic transformation of the variance domain is proposed as a remedy.

Overall, we conclude that the approach using the Green's function in all test cases convinces through its simplicity of implementation and its low computational runtimes. The disadvantage is that it is not straightforward to extend the approach to the pricing to American or other types of compound options as it is possible for the sparse grid method. Furthermore, although for the FRFT technique and the transition density approach the further development to pricing compound options under Heston model dynamics with stochastic interest rates might be possible to achieve, the runtimes of the two methods will likely no longer compare as favorably against the runtimes of the

sparse grid method and the Monte Carlo simulations. Under these conditions, the sparse grid method obviously represents a genuine alternative to Monte Carlo simulations.

8. Conclusion

We have implemented a number of different techniques to evaluate European compound option prices under Heston stochastic volatility dynamics. Each method has its own advantages and disadvantages. Comparing both the efficiency and accuracy of the different methods through a number of numerical examples, we found that the Green's function approach is both easy to implement and produces a small number of option prices fairly quickly. The sparse grid approach is good at producing a large number of prices with an acceptable accuracy and within a reasonable time frame although the implementation of the sparse grid approach requires the use of parallel computing on a number of cluster nodes. The fractional fast Fourier transform method compares better with respect to accuracy and computational runtime than the sparse grid approach, but does not offer the flexibility to easily advance the method to price more involved types of compound options. We also implemented the Monte Carlo simulation for comparison purposes. The Monte Carlo sampling technique is relatively easy to implement, but needs a large number of paths to get a relatively accurate price. We have improved the efficiency of the Monte Carlo approach by using the parfor-loop in Matlab to compute different blocks of paths in parallel. In the above approaches, it is relatively easy to generalize the sparse grid approach to handle compound options with early exercise features while other approaches may have some limitations in this regard.

9. Appendix

The characteristic function of x_{T_M} and v_{T_M} under the risk-neutral measure is given by

$$\begin{aligned}\varphi_{x,v}(u_x,u_v) &= \exp\left(iu_x x_0 + iu_x(r_d-r_f)T - iu_x\frac{\rho}{\sigma}v_0 - iu_x\frac{\rho}{\sigma}\kappa\theta T\right)\\ &\quad\times\exp\left(A(T,a,b)v_0 + B(T,a,b)\right),\end{aligned}$$

with

$$\begin{aligned}a &= iu_v + iu_x\frac{\rho}{\sigma},\\ b &= -\frac{\kappa\rho}{\sigma}iu_x + \frac{1}{2}iu_x + \frac{1}{2}u_x^2(1-\rho^2),\end{aligned}$$

and

$$\begin{aligned} A(\tau,a,b) &= \frac{-(1-\exp(-d\tau)(2b+\kappa a)+da(1+\exp(-d\tau))}{\gamma}, \\ B(\tau,a,b) &= \frac{\kappa\theta}{\sigma^2}(\kappa-d)\tau+\frac{2\kappa\theta}{\sigma^2}\ln\frac{2d}{\gamma}, \\ d &= \sqrt{\kappa^2+2\sigma^2 b}, \\ \gamma &= 2d\exp(-d\tau)+(\kappa+d-\sigma^2 a)(1-\exp(-d\tau)). \end{aligned}$$

Using the definitions for the functions A and B above, the function h under the risk-neutral measure is given by

$$\begin{aligned} h(u,v,z) &= -\frac{1}{m^\mu}\exp\left(i(u+z)x_0-i(u+z)\frac{\rho}{\sigma}v_0+iu(r-q)T_M+iz(r-q)T_D\right) \\ &\quad\times\exp\left(\frac{\kappa\theta}{\sigma^2}(\kappa-d_{uz})T_D-iu\frac{\rho}{\sigma}\kappa\theta T_M-iz\frac{\rho}{\sigma}\kappa\theta T_D+B(T_D-T_M,a_z,b_z)\right) \\ &\quad\exp\left(\frac{(d_{uz}e^+-\kappa e^-)v_0}{2nd_{uz}}\right)F_{\chi'^2_{df}(c)}\left(-2\frac{m}{n}v\right)+R, \end{aligned}$$

where

$$\begin{aligned} a_z &= iz\frac{\rho}{\sigma}, \\ b_z &= \frac{1}{2}iz-iz\frac{\rho\kappa}{\sigma}+\frac{1}{2}z^2(1-\rho^2), \\ a_{uz} &= iu\frac{\rho}{\sigma}+A(T_D-T_M,a_z,b_z), \\ b_{uz} &= \frac{1}{2}i(u+z)-i(u+z)\frac{\rho\kappa}{\sigma}+\frac{1}{2}(u+z)^2(1-\rho^2), \\ d_{uz} &= \sqrt{\kappa^2+2\sigma^2 b_{uz}}, \\ e^\pm &= 1\pm\exp(-d_{uz}T_M), \end{aligned}$$

and

$$\begin{aligned} m &= \frac{d_{uz}e^+ + \kappa e^- - \sigma^2 e^- a_{uz}}{2d_{uz}}, \\ n &= \frac{-\sigma^2 e^-}{2d_{uz}}, \\ c &= 2\frac{(d_{uz}e^+-\kappa e^-)\left(a_{uz}-\frac{m}{n}\right)-2e^- b_{uz}}{2d_{uz}m}v_0. \end{aligned}$$

The term R denotes the residual of the function h. The function F denotes the cumulative distribution function for non-central chi-squared random variables with $df=\frac{4\kappa\theta}{\sigma^2}$ degrees of freedom, non-centrality parameter c and complex arguments.

The function h can be computed by using the above definition with a third argument of $z - i$ and multiplying with a factor equal to $\exp(-(r-q)T_D - x_0)$ to account for the measure change to $\mathbb{Q}_S$.

References

Black, F. & Scholes, M. (1973), 'The Pricing of Corporate Liabilites', *Journal of Political Economy* **81**, 637–659.

Carr, P. & Madan, D. (1999), 'Option Valuation Using the Fast Fourier Transform', *Journal of Computational Finance* **2**(4).

Chiarella, C., Ziogas, A. & Ziveyi, J. (2010), Representation of American Option Prices Under Heston Stochastic Volatility Dynamics Using Integral Transforms, *in* C. Chiarella & A. Novikov, eds, 'Contemporary Quantitative Finance', Springer.

Chourdakis, K. (2005), 'Option Pricing Using the Fractional FFT', *Journal of Computational Finance* **8**(2).

Dempster, M. & Hong, S. (2002), Spread Option Valuation and the Fast Fourier Transform, *in* H. Geman, D. Madan & S. R. Pliska, eds, 'Proceedings of the 1st World Congress of the Bachelier Finance Society', Springer.

Ekstrom, E., Lotstedt, P. & Tysk, J. (2009), 'Boundary Values and Finite Difference Methods for the Single Factor Term Structure Equation', *Applied Mathematical Finance* **16**(3), 253–259.

Fang, F. & Oosterlee, C. (2008), 'A Novel Pricing Method for European Options Based on Fourier-Cosine Series Expansions', *SIAM J. Sci. Comput.* **31**(2), 826–848.

Fang, F. & Oosterlee, C. (2011), 'A Fourier-Based Valuation Method for Bermudan and Barrier Options under Heston's Model', *SIAM J. Financial Math* **2**, 439–463.

Geske, R. (1979), 'The Valuation of Compound Options', *Journal of Financial Economics* **7**, 63–81.

Geske, R. & Johnson, H. E. (1984), 'The American Put Option Valued Analytically', *Journal of Finance* **39**, 1511–1524.

Griebsch, S. (2012), The Evaluation of European Compound Option Prices under Stochastic Volatility using Fourier Transform Techniques. Accepted for publication in Review of Derivatives Research, DOI: 10.1007/s11147-012-9083-z.

Heston, S. (1993), 'A Closed-Form Solution for Options with Stochastic Volatility with Applications to Bond and Currency Options', *Review of Financial Studies* **6**(2), 327–343.

Ikonen, S. & Toivanen, J. (2007), 'Componentwise Splitting Methods for Pricing American Options under Stochastic Volatility', *International Journal of Theoretical and Applied Finance* **10**(2), 331–361.

Lipton, A. (2001), *Mathematical Methods for Foreign Exchange*, World Scientific, Singapore.

Lord, R., Koekkoek, R. & Dijk, D. V. (2010), 'A Comparison of Biased Simulation Schemes for Stochastic Volatility Models', *Quantitative Finance* **10**(2), 177–194.

Reisinger, C. (2004), Numerische Methoden für hochdimensionale parabolische Gleichungen am Beispiel von Optionspreisaufgaben, PhD thesis, Universitt Heidelberg.

Reisinger, C. & Wittum, G. (2007), 'Efficient Hierarchical Approximation of High-Dimensional Option Pricing Problems', *SIAM Journal on Scientific Computing* **29**(1), 440–458.

Seong, Y. (2002), 'Analytic Valuation of Compound Options. In volatility: New Estimation Techniques for Pricing Derivatives', *BMO Nesbitt Burns* .

Shephard, N. (1991), 'From Characteristic Function to Distribution Function: A Simple Framework for the Theory', *Econometric Theory* **7**(4), 519–529.